Charge compensation effect in $Pr_{1-y}Sr_yFe_{1-x}Co_xAsO$ codoped with Sr and Co

X. Lin, H. J. Guo, C. Y. Shen, Y. K. Luo, Q. Tao, G. H. Cao, and Z. A. Xu*

State Key Laboratory of Silicon Materials and Department of Physics, Zhejiang University, Hangzhou 310027, People's Republic of China

(Received 18 July 2010; revised manuscript received 10 December 2010; published 12 January 2011)

Superconductivity of polycrystalline Sr and Co codoped $Pr_{1-y}Sr_yFe_{1-x}Co_xAsO$ samples was investigated by measuring resistivity, dc magnetic susceptibility, thermopower, and Hall effect. In the $PrFe_{1-x}Co_xAsO$ samples with only Co doping, T_c reaches a maximum of 16 K at $x = 0.075$–0.1, and the variation of T_c with Co content (x) is a dome-shaped curve. In the Co and Sr codoped $Pr_{0.8}Sr_{0.2}Fe_{1-x}Co_xAsO$ system, the phase diagram separates into two regions. The thermopower and Hall data indicate that the hole-type charge carrier dominates in the low Co doping region ($x \leqslant 0.075$) and the system becomes electron type in the high Co doping region ($x \geqslant 0.075$). T_c first decreases with increasing Co content to a lowest T_c of 3.5 K at $x = 0.075$, then it increases and reaches a maximum of ~16 K at $x = 0.15$. The transition from hole-type to electron-type superconductivity in the nominal $Pr_{0.8}Sr_{0.2}Fe_{1-x}Co_xAsO$ system around $x = 0.075$ implies that the charge-carrier density is one of the decisive factors to control superconductivity.

DOI: 10.1103/PhysRevB.83.014503 PACS number(s): 74.70.Dd, 74.62.Dh, 74.25.Dw, 74.25.F–

I. INTRODUCTION

Following the discovery of superconductivity in electron-doped oxypnictide $LaFeAsO_{1-x}F_x$ (Ref. 1) with ZrCuSiAs-type structure (also called 1111 phase), the superconducting (SC) critical temperature (T_c) was soon raised beyond the theoretical limit (40 K) predicted from the Bardeen-Cooper-Schrieffer (BCS) theory in several electron-type doping systems.[2–5] Meanwhile, superconductivity was also observed in the Sr-doped hole-type $La_{1-x}Sr_xFeAsO$ system.[6] However, in the 1111 phase family, superconductivity induced by hole-type doping was only achieved in a few compounds,[6–9] and there were controversial reports on the hole-type 1111 phase superconductors.[1,6,10] On the other hand, superconductivity can be easily induced by electron-type doping whether the dopants are outside the FeAs layer or within the conducting FeAs layer.[2,3,5,11–17] For example, the partial substitution of Fe by Co or Ni can induce extra itinerant electrons into the oxypnictides and a domelike doping dependence of T_c is established,[12,13] which is consistent with the results of band calculations.[18] Furthermore, the similar domelike doping dependence of T_c and the occurrence of superconductivity at the verge of the antiferromagnetic (AFM) phase in both iron pnictides and cuprates strongly suggest that the two high-T_c superconducting families should share some universal underlying physics. It is believed that the magnetism of Fe ions in the parent compounds should play a crucial role in the mechanism of high-T_c superconductivity. According to the measurements of angle-resolved photoemission spectra (ARPES),[19,20] multiple isotropic superconducting gaps were observed in the iron pnictides, and a scenario of $s\pm$ wave pairing symmetry is further proposed theoretically.[21–24] In this scenario, the relative phases of the SC order parameters in hole or electron pockets is opposite, which is determined by the Josephson coupling between these pockets. A particular interesting issue is the comparison of the phase diagrams for hole and electron doping in 1111 phase pnictides. In contrast to the d-wave high-T_c cuprates where the parent compounds are AFM Mott insulators and a universal dependence of T_c on charge-carrier doping is established,[25] it is still an open issue whether the charge-carrier density is a universal parameter to control superconductivity in FeAs-based SC pnictides with various chemical doping approaches.

In this paper, we investigate superconductivity of the Sr and Co codoped $Pr_{1-y}Sr_yFe_{1-x}Co_xAsO$ system by measuring resistivity, magnetic susceptibility, thermopower, and Hall effect. In the only Co-doped $PrFe_{1-x}Co_xAsO$, T_c reaches a maximum of 16 K at an optimal doping level of $x = 0.075$–0.1, and the variation of T_c with Co content (x) is a dome-shaped curve, similar to the case of the Co-doped LaFeAsO and SmFeAsO systems.[12] According to a previous report,[8] 20% Sr doped onto the Pr site is near the optimal doping level in the $Pr_{0.8}Sr_{0.2}FeAsO$ samples, so we chose 20% Sr doping in our study. In the Co and Sr codoped $Pr_{0.8}Sr_{0.2}Fe_{1-x}Co_xAsO$ system, the T_c-x phase diagram separates into two regions in which electron- and hole-type charge carriers dominate, respectively, and the optimal doping level shifts to a higher Co content x of 0.15 with nearly the same maximum T_c of 16 K in the electron-type region. Our results indicate that there is an obvious compensation effect between the electron-type and hole-type dopants and the charge-carrier density should be one of the decisive factors to control superconductivity in the oxypnictide superconductors.

II. EXPERIMENT

Polycrystalline samples of $Pr_{1-y}Sr_yFe_{1-x}Co_xAsO$ were synthesized by solid-state reaction in vacuum using powders of PrAs, SrAs, Pr_6O_{11}, FeAs, CoAs, and Fe. PrAs, FeAs, and CoAs were presynthesized similarly to our previous report.[12] SrAs was prepared by reacting stoichiometric Sr pieces and As powders at 873 K for 10 h and then at 1123 K for 10 h. All the starting materials are of high purity (⩾99.9%). The powders of these intermediate materials were weighed according to the stoichiometric amounts of $Pr_{1-y}Sr_yFe_{1-x}Co_xAsO$ ($y = 0$, 0.2 and $x = 0$–0.3), thoroughly mixed in an agate mortar, and then pressed into pellets under a pressure of 2000 kg/cm^2. These processes were performed in a glove box filled with high-purity argon. The pellets were sealed in evacuated quartz tubes, heated uniformly at 1173 K for 5 h and then at 1433 K for 40 h, and finally furnace cooled to room temperature.

Powder x-ray diffraction (XRD) was performed at room temperature using a D/Max-rA diffractometer with Cu-K_α radiation. Lattice parameters were refined by a least-squares fit using at least 20 peaks with 2θ from 10° to 80°. The electrical resistivity was measured using a standard four-terminal method. The thermopower was measured by using a steady-state technique. All the measurements of transport properties were carried out on a Quantum Design physical property measurement system (PPMS-9). The measurements of dc magnetic properties were performed on a Quantum Design magnetic property measurement system (MPMS-5).

III. RESULTS AND DISCUSSION

A. Superconductivity in $PrFe_{1-x}Co_xAsO$

Figure 1 shows the room-temperature powder XRD patterns for the $PrFe_{1-x}Co_xAsO$ samples with only Co doping. Almost all the XRD peaks can be indexed based on a tetragonal cell with the space group of $P4/nmm$. Only tiny Pr_2O_3 and FeAs impurities are detected in several samples. The inset of Fig. 1 shows the calculated lattice parameters as functions of Co content. It can be found that the c axis decreases monotonously with increasing x, but the a axis does not change very much. This result is consistent with the previous reports on the Co-doped 1111 phase such as $RFe_{1-x}Co_xAsO$ (R = La, Sm),[11,12] indicating that Co ions have been successfully doped onto the Fe sites.

The temperature dependence of resistivity for $PrFe_{1-x}Co_xAsO$ is shown in Fig. 2(a). The inset of Fig. 2(a) plots the zoom-in resistivity behavior in the temperature range of 2–30 K. For the parent compound PrFeAsO, a small anomaly occurs around 12 K due to AFM phase transition of Pr^{3+} ions.[26] Another obvious anomaly is observed around 140 K in resistivity, which should result from the structural and AFM phase transitions of FeAs layers, according to the studies of neutron scattering.[26,27] Upon Co doping in $PrFe_{1-x}Co_xAsO$, the anomaly in resistivity is suppressed to about 80 K with 2.5% Co doping, and superconductivity appears as $x \geqslant 0.05$. The SC critical temperature $T_c^{\rm mid}$ (defined as the midpoint in the resistive transition) reaches a maximum of 16 K around $x = 0.075$–0.1, consistent with

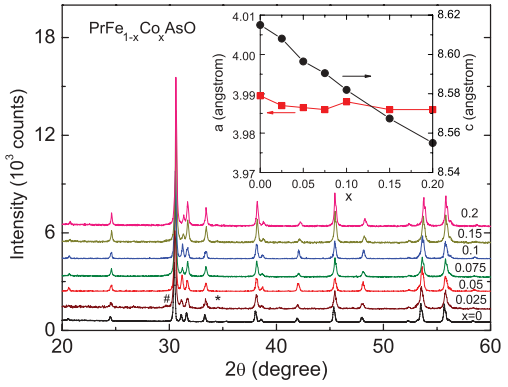

FIG. 1. (Color online) Powder x-ray-diffraction patterns at room temperature for $PrFe_{1-x}Co_xAsO$ ($x = 0.0$–0.2). Tiny impurities of Pr_2O_3, FeAs are labeled by #, ⋆, respectively. The inset plots the lattice parameters a and c as functions of Co content.

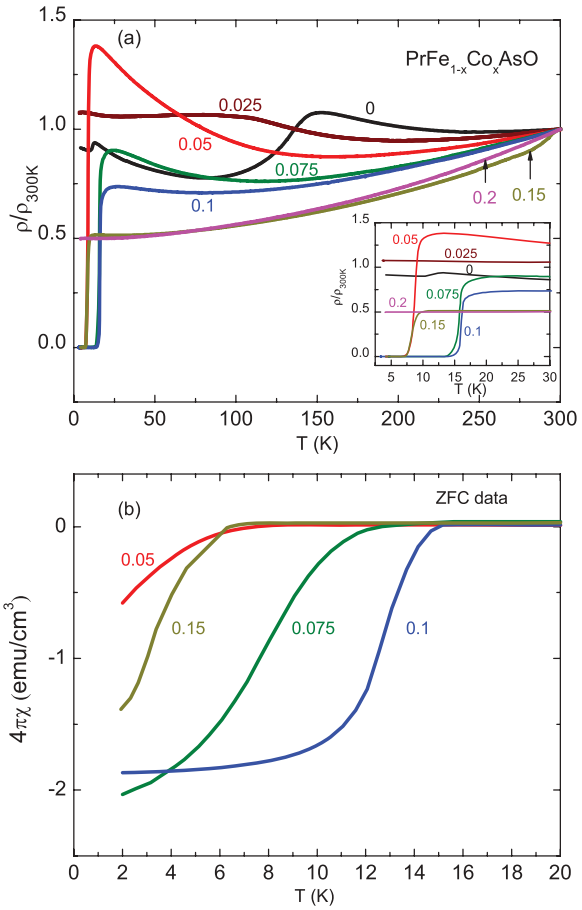

FIG. 2. (Color online) (a) Temperature dependence of resistivity for $PrFe_{1-x}Co_xAsO$ samples. The inset shows the resistivity in the temperature range of 2–30 K. (b) dc magnetic susceptibility data of zero-field cooling (ZFC) for several $PrFe_{1-x}Co_xAsO$ samples, measured under H of 10 Oe.

the previous report of $PrFe_{1-x}Co_xAsO$ synthesized under high pressure.[28] Another group reported a highest T_c of 14 K for $PrFe_{1-x}Co_xAsO$,[29] a little lower than the T_c value of our samples. Please note that the dependence of resistivity on temperature is nonlinear even at the optimaly doping level ($x = 0.1$). With further Co doping, superconductivity is suppressed, and finally vanishes at $x = 0.2$. Figure 2(b) shows the dc magnetic susceptibility (χ) for $PrFe_{1-x}Co_xAsO$ samples, indicating bulk superconductivity. Because the demagnetization effect is not taken into account, some of the observed volume magnetic screening ratio could even exceed 100%.

Figure 3 shows the temperature dependence of thermopower (S) for the $PrFe_{1-x}Co_xAsO$ samples. An upturn in S of the parent compound PrFeAsO occurs around 140 K, consistent with the anomaly in the resistivity due to the structural and magnetic phase transition. With Co doping, the anomaly is suppressed and thermopower becomes more negative, which indicates that Co dopant introduces electron-type charge carriers. It should be mentioned that the isovalent Ru doping in the $PrFe_{1-x}Ru_xAsO$ systems also leads to a negative thermopower.[30] The absolute value of thermopower ($|S|$) is enhanced around the optimal doping level ($x = 0.075$–0.1),

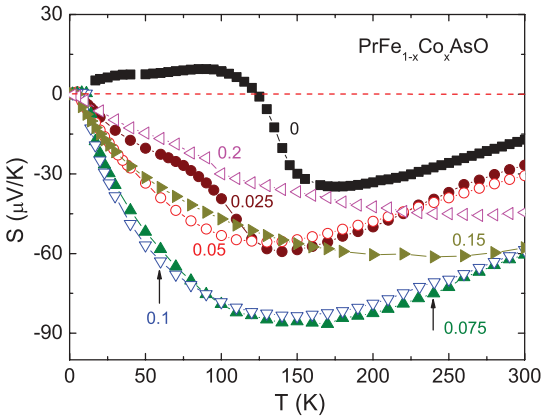

FIG. 3. (Color online) Temperature dependence of thermopower for the $PrFe_{1-x}Co_xAsO$ samples.

suggesting that there is a correlation between T_c and the absolute value of thermopower. Such a correlation has also been proposed in other Co-doped 1111 phase samples.[12] As the Co content increases further beyond the optimal doping level, $|S|$ decreases gradually and its temperature dependence becomes usual metal like.

B. Superconductivity in $Pr_{0.8}Sr_{0.2}Fe_{1-x}Co_xAsO$

Figure 4 shows the XRD patterns for the $Pr_{0.8}Sr_{0.2}Fe_{1-x}Co_xAsO$ samples. Most peaks can be indexed based on a tetragonal cell with the space group of $P4/nmm$ for all the Co and Sr codoped samples. However, small amounts of Pr_2O_3, FeAs, and $SrFe_2As_2$ impurities appear in the XRD patterns once Sr is doped. Such impurity phases are often observed in the Sr-doped 1111 phase samples according to the previous reports,[8] which implies that not all the Sr ions have been substituted for Pr ions. Indeed, the measurement of energy-dispersive x-ray spectroscopy (EDX) spectra reveals that the Sr content in the grains of the nominal $Pr_{0.8}Sr_{0.2}Fe_{1-x}Co_xAsO$ samples is between 0.10 and 0.13, less than 0.2, and it does not change much with the Co content. The inset shows the calculated lattice parameters as

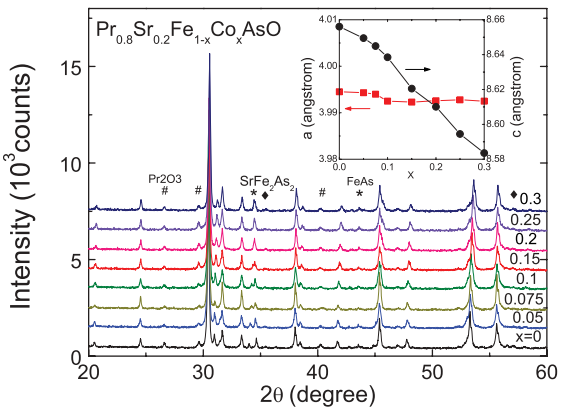

FIG. 4. (Color online) Powder x-ray-diffraction patterns at room temperature for $Pr_{0.8}Sr_{0.2}Fe_{1-x}Co_xAsO$ with $x = 0.0$–0.3. Some impurities of Pr_2O_3, FeAs, and $SrFe_2As_2$ are labeled by #, ⋆, ♦, respectively. The inset plots the lattice parameters versus cobalt content (x).

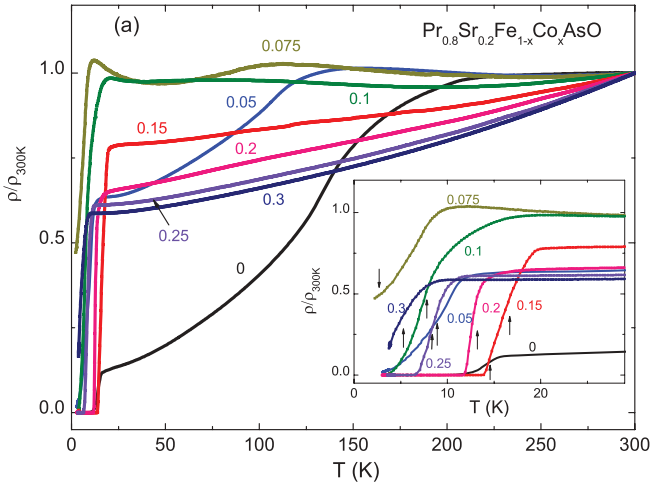

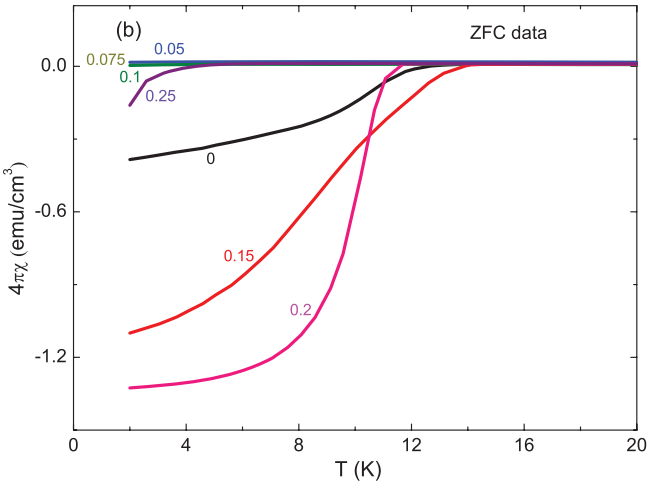

FIG. 5. (Color online) (a) Temperature dependence of resistivity for the $Pr_{0.8}Sr_{0.2}Fe_{1-x}Co_xAsO$ samples. The inset shows the resistivity in the temperature range of 2–30 K and the midpoint in the resistive transition has been labeled by vertical arrows. (b) dc magnetic susceptibility data of zero-field cooling (ZFC) for several $Pr_{0.8}Sr_{0.2}Fe_{1-x}Co_xAsO$ samples, measured under H of 10 Oe.

functions of Co content (x). The c axis decreases linearly with increasing x and the a axis again does not change very much, similar to that of $PrFe_{1-x}Co_xAsO$. Comparing the lattice parameters between the $PrFe_{1-x}Co_xAsO$ and $Pr_{0.8}Sr_{0.2}Fe_{1-x}Co_xAsO$ samples, the a axis increases by about 0.17% and the c axis increases by about 0.6%, respectively, due to Sr doping.

The temperature-dependent resistivity of the $Pr_{0.8}Sr_{0.2}Fe_{1-x}Co_xAsO$ samples is shown in Fig. 5(a). The SC critical temperature T_c^{mid} for $Pr_{0.8}Sr_{0.2}FeAsO$ with only Sr doping is about 14 K, comparable to the previous result.[8] Upon Co doping, T_c^{mid} decreases first to about 3.5 K at $x = 0.075$, which is much lower than T_c of ~16 K for the only Co-doped $PrFe_{0.925}Co_{0.075}AsO$. Then T_c^{mid} increases from 3.5 K with increasing Co doping and finally reaches a second maximum of about 16 K at $x = 0.15$. Please note that the maximum T_c^{mid} of the Sr and Co codoped system is almost the same as that of the $PrFe_{0.9}Co_{0.1}AsO$ system. Upon further Co doping, T_c^{mid} starts to decrease, indicating that the system enters into the overdoped regime. However, superconductivity

does not vanish when x is as large as 0.3. The enlarged plot of resistivity in the temperature range of 2–30 K is also shown in the inset of Fig. 5.

There is an anomalous decrease in resistivity as temperature is below 150 K for the $Pr_{0.8}Sr_{0.2}FeAsO$ sample. Such an anomalous behavior in resistivity is often observed in Sr-doped hole-type 1111 phase superconductors.[6,8,9] Upon Co doping, this anomaly is suppressed, but it is still observable for $x \leqslant 0.075$ in the $Pr_{0.8}Sr_{0.2}Fe_{1-x}Co_xAsO$ samples. With further Co doping, this anomaly finally disappears and the resistivity becomes Fermi-liquid like in the overdoped regime, similar to that of overdoped $PrFe_{1-x}Co_xAsO$ systems; we will show hereafter that the system becomes electron type as $x > 0.075$. The origin of this anomaly is not well understood at present. Apparently this behavior is reminiscent of the structural and AFM phase transition in the parent compound PrFeAsO. However, we argue that this anomaly could not result from the AFM order of FeAs layers based on the following facts. First, the anomaly in $Pr_{0.8}Sr_{0.2}FeAsO$ occurs over 150 K, which is even higher than the AFM transition temperature (around 140 K) of the parent compound PrFeAsO. Second, such a hump in resistivity could be a common feature in both 1111 and 122 hole-doped pnictide superconductors. For the K-doped 122 phase $Ba_{1-x}K_xFe_2As_2$, there is a convex in resistivity at low temperature, similar to the anomaly in the hole-type 1111 phase, for almost all of the doping range (from underdoped to overdoped).[31–33] Previous studies have confirmed that the AFM order of Fe ions disappears in the optimal doping and overdoping regimes of $Ba_{1-x}K_xFe_2As_2$.[34,35]

Figure 5(b) plots the dc magnetic susceptibility (χ) of zero-field cooling (ZFC) under the measurement field of 10 Oe for the superconducting $Pr_{0.8}Sr_{0.2}Fe_{1-x}Co_xAsO$ samples. It seems that the value of the SC magnetic screening volume ratio ($4\pi\chi$) is related to T_c. Bulk superconductivity can be confirmed near the optimal level. Moreover, the magnetic screening volume ratio of some samples even exceeds 100% owing to the demagnetization effect. The value of the SC magnetic screening volume ratio is nearly zero around $x = 0.075$, which has the lowest T_c^{mid} determined from the resistivity.

Figure 6 shows the temperature dependence of thermopower (S) for the $Pr_{0.8}Sr_{0.2}Fe_{1-x}Co_xAsO$ samples. A positive thermopower for $Pr_{0.8}Sr_{0.2}FeAsO$ with only Sr dopant indicates that Sr is indeed an effective hole-type dopant. For the samples with low Co doping content ($x \leqslant 0.075$), although the thermopower remains positive, the S value decreases obviously with increasing Co content. With further Co dopant ($x \geqslant 0.1$), the thermopower becomes negative and the absolute value of $|S|$ reaches a maximum around the optimal doping level of $x = 0.15$. The enhancement of $|S|$ at the optimal doping level is also observed in the only Co-doped 1111 systems.[12] The transition from hole type to electron type in S occurs around $x = 0.075$. In the hole-type side, there is a broad peak in thermopower, which locates at around 150 K for $Pr_{0.8}Sr_{0.2}FeAsO$ and moves to lower temperature with Co doping. The broad peak in S coincides with the anomalous sharp drop in the resistivity of the same samples [see Fig. 5(a)], suggesting that there might be a subtle change in the electronic structure in the hole-type 1111 phase. However, it has not been understood well.

The evolution of S with x may be explained by a two-band model: $S = \frac{\sigma_h|S_h| - \sigma_e|S_e|}{\sigma_h + \sigma_e}$; $\sigma_{e,h}$ represents the electron and hole conductivity, respectively, and $|S_{e,h}|$ represents the absolute value of thermopower for the electron and hole, respectively. Co doping introduces an electron-type charge carrier which leads to an increase in the $\sigma_e|S_e|$ term and the total thermopower (S) becomes more negative. The evolution of thermopower with x suggests that the dominant charge carrier is changed from hole type into electron type at around $x = 0.075$. Because the actual content of Sr is less than 0.20 in the nominal $Pr_{0.8}Sr_{0.2}Fe_{1-x}Co_xAsO$ samples according to the EDX result, it is reasonable that about 7.5% of the electron-type dopant (Co doping) can almost compensate for the hole-type dopant (Sr doping).

The results of the Hall effect shown in Fig. 7 further confirm that Sr is a hole-type dopant and Co is electron type in the Co and Sr codoped system. However, the Hall coefficient (R_H) is negative above 200 K for even only Sr-doped $Pr_{0.8}Sr_{0.2}FeAsO$ and then it increases sharply and becomes positive at low temperature. Such a R_H behavior is observed for all the Sr-doped 1111 phase superconductors.[6,8,9] With Co doping, the temperature at which the sign of R_H changes is suppressed to lower temperatures for the low Co doping level ($x \leqslant 0.05$) and finally R_H becomes negative for the whole temperature range in the higher Co dopant region (i.e., $x = 0.15$). The sign change in R_H for $x = 0$, 0.05, and 0.075 also coincides

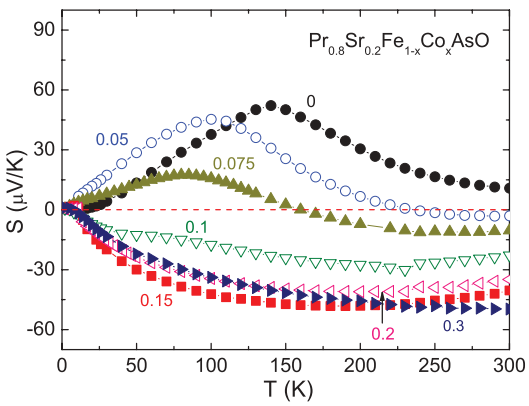

FIG. 6. (Color online) Temperature dependence of thermopower of $Pr_{0.8}Sr_{0.2}Fe_{1-x}Co_xAsO$ samples.

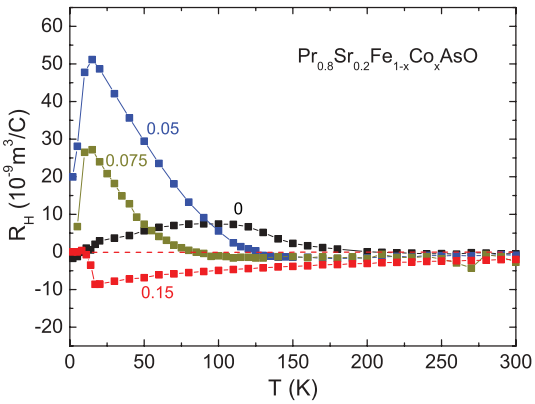

FIG. 7. (Color online) Temperature dependence of Hall coefficient (R_H) for the $Pr_{0.8}Sr_{0.2}Fe_{1-x}Co_xAsO$ samples. R_H is measured under $\mu_0 H$ of 5 T.

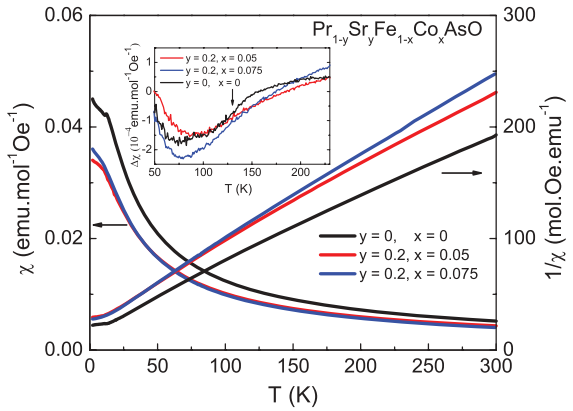

FIG. 8. (Color online) dc magnetic susceptibility (χ) and $1/\chi$ for $Pr_{0.8}Sr_{0.2}Fe_{1-x}Co_xAsO$ samples with $x = 0.05$ and 0.075. Measurements were performed under the field of 1000 Oe. The inset shows the residual dc magnetic susceptibility (χ) by subtracting the Curie-Weiss bachground of Pr ions. The arrow indicates the magnetic phase transition around 135 K for PrFeAsO.

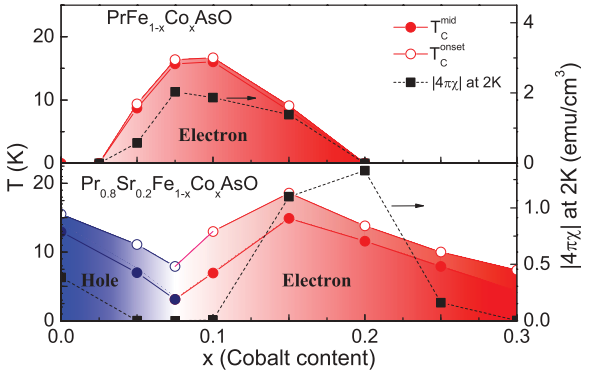

FIG. 9. (Color online) Co content (x) dependence of superconducting critical temperature at the midpoint and onset point of the resistive transition ($T_c^{\rm mid}$ and $T_c^{\rm onset}$) and SC magnetic screening volume ratio ($-4\pi\chi$) at 2 K for the $PrFe_{1-x}Co_xAsO$ and $Pr_{0.8}Sr_{0.2}Fe_{1-x}Co_xAsO$ samples. $T_c^{\rm mid}$ and $T_c^{\rm onset}$ are labeled by solid and open circles, respectively, and $-4\pi\chi$ is labeled by solid squares.

with the anomalous drop in resistivity and the broad peak in thermopower.

Figure 8 shows the dc magnetic susceptibility (χ) and its reciprocal ($1/\chi$) for the parent compound PrFeAsO and the $Pr_{0.8}Sr_{0.2}Fe_{1-x}Co_xAsO$ samples with $x = 0.05$ and 0.075. A small kink in χ occurs at T_N(Pr) of about 12 K due to the AFM order of Pr^{3+} ions. For $T > T_N$(Pr), $1/\chi$ behaves linearly with T, which confirms the Curie-Weiss paramagnetic behavior. By fitting the dc magnetic susceptibility (χ) to the Curie-Weiss law, we obtain that the effective magnetic moment $p_{\rm eff}$ is $3.39\mu_B$/f.u. for PrFeAsO, which is a little smaller than the theoretical value of free Pr^{3+} ions. With Co doping in the $Pr_{0.8}Sr_{0.2}Fe_{1-x}Co_xAsO$ samples, the effective magnetic moment $p_{\rm eff}$ becomes even smaller, which is $3.19\mu_B$/f.u. for $x = 0.05$ and $3.22\mu_B$/f.u. for $x = 0.075$, respectively. In order to distinguish the magnetic phase transition related to the Fe ions in the parent compound PrFeAsO, we subtract the susceptibility data by the Curie-Weiss background term originating from Pr ions (see the inset of Fig. 8) and thus we observe a magnetic phase transition around 135 K, consistent with the transition in the resistivity for the same sample (see Fig. 2). But for the $Pr_{0.8}Sr_{0.2}Fe_{1-x}Co_xAsO$ samples with $x = 0.05$ and 0.075, such a transition is not obvious in the subtracted dc magnetic susceptibility data. Although there are some anomalous changes in resistivity, thermopower, and Hall coefficient of the samples with $x = 0.05$ and 0.075, we have argued that these changes are similar to the anomaly in the transport properties of K-doped 122 phase samples $Ba_{1-x}K_xFe_2As_2$ (even in optimal doping and overdoping regimes),[32,33] and they should not result from the AFM order of Fe ions. Thus we cannot confirm whether the structural and magnetic phase transition of Fe ions is restored or at $x = 0.075$, at which electron-type Co dopant should almost compensate for the hole-type Sr dopant in the $Pr_{0.8}Sr_{0.2}Fe_{1-x}Co_xAsO$ samples. We proposed that the anomalous behavior in the transport properties of $Pr_{0.8}Sr_{0.2}Fe_{1-x}Co_xAsO$ ($x \leqslant 0.075$) may be related to electronic structure, especially the multiple conducting bands. Higher quality samples and more investigations are required to clarify the nature of this anomalous behavior in the transport properties.

The phase diagram for both $PrFe_{1-x}Co_xAsO$ and $Pr_{1-y}Sr_yFe_{1-x}Co_xAsO$ systems are summarized in Fig. 9. In addition to $T_c^{\rm mid}$ data, $T_c^{\rm onset}$ (defined at the point of 90% value in the resistive transition) is also shown in the graph, and it evolves with Co content similar to that of $T_c^{\rm mid}$ for both systems. The superconducting region for the $PrFe_{1-x}Co_xAsO$ system is domelike between about $x = 2.5\%$ and 20%. The maximum $T_c^{\rm mid}$ of 16 K occurs at $x = 0.075$–0.10. The right overdoped region is obviously larger than the underdoped region. Sr doping in the $Pr_{0.8}Sr_{0.2}Fe_{1-x}Co_xAsO$ system divides the T_c-x dome into two different regions (shown as different colors in the lower panel of Fig. 9). In the left region with low Co content ($x \leqslant 0.075$), $T_c^{\rm mid}$ is suppressed from a maximum of 16 K at $x = 0$ to a minimum of 3.5 K at the transition point $x = 0.075$. A hole-type charge carrier dominates in this region according to the data of thermopower and Hall effect. In the right region with high Co content ($x > 0.075$), an electron-type charge carrier dominates. Compared to the phase diagram of only the Co-doped $PrFe_{1-x}Co_xAsO$ system, the T_c-x dome shifts to the higher Co content region by about 7.5% Co content (x) due to the 20% Sr doping. The maximum $T_c^{\rm mid}$ of 16 K also moves to higher x of 0.15. Considering that the actual Sr content is less than 0.20 in the nominal $Pr_{0.8}Sr_{0.2}Fe_{1-x}Co_xAsO$ samples, it is reasonable that Sr doping can compensate for about 7.5% of electron-type doping in the Sr and Co codoped system. However, the electron-dominant superconducting region of $Pr_{0.8}Sr_{0.2}Fe_{1-x}Co_xAsO$ extends to much higher Co doping level ($x \geqslant 0.3$) compared to $PrFe_{1-x}Co_xAsO$. Roughly speaking, after subtracting the compensated electron doping level, i.e., using $x = 0.075$ as the effective electron doping level, the phase diagram of $Pr_{0.8}Sr_{0.2}Fe_{1-x}Co_xAsO$ in the electron-type side is essentially the same as the phase diagram of $PrFe_{1-x}Co_xAsO$. This finding indicates that the charge-carrier density is one of the decisive factors to control high-T_c superconductivity in FeAs-based pnictides in spite of different chemical doping methods. We also plot the SC magnetic screening volume ratio ($-4\pi\chi$) versus Co content at 2 K in Fig. 9. It behaves

similarly to that of T_c for both systems. The samples near the optimal doping level have the largest magnetic screening volume ratio. When T_c comes down to lower temperature, the magnetic screening volume ratio decreases quickly. Especially for the $Pr_{0.8}Sr_{0.2}Fe_{1-x}Co_xAsO$ samples around $x = 0.075$, the magnetic screening volume ratio is almost zero, indicating the absence of bulk superconductivity at $x = 0.075$. As we mentioned in the above, 7.5% Co doping almost compensates the Sr doping in this system, and the restoration of the structural and magnetic transitions of FeAs layers should be expected. However, we could not confirm whether there is such a restoration based on our present data.

IV. CONCLUSION

In summary, we have synthesized the Sr and Co codoped $Pr_{1-y}Sr_yFe_{1-x}Co_xAsO$ samples. The thermopower and Hall data confirm that the hole-type carriers are induced by Sr dopants and the electron-type carriers are induced by Co dopants. Compared to the only Co-doped $PrFe_{1-x}Co_xAsO$ system, nominally 20% Sr doping causes splitting of the T_c-x phase diagram into two different regions in the $Pr_{0.8}Sr_{0.2}Fe_{1-x}Co_xAsO$ system. There is a transition from the low Co content hole-type region to the high Co content electron-type region around $x = 0.075$. However, the maximum T_c in the two different regions is almost the same. Furthermore, if we use the effective electron doping level ($x = 0.075$), the phase diagram of the Sr and Co codoped system in the electron-type side is essentially the same as that of the only Co-doped system. There is always an anomaly in the normal-state transport properties of hole-type $Pr_{0.8}Sr_{0.2}Fe_{1-x}Co_xAsO$ samples, and its origin is still an open question. Our results suggest that the charge-carrier density could be one of the decisive factors to control superconductivity in pnictide superconductors.

ACKNOWLEDGMENTS

We gratefully acknowledge support from the NSF of China (Contracts No. 10634030 and No. 10931160425), National Basic Research Program of China (Contract No. 2007CB925001), and the Fundamental Research Funds for the Central Universities of China (Program No. 2010QNA3026).

*zhuan@zju.edu.cn

[1] Y. Kamihara, T. Watanabe, M. Hirano, and H. Hosono, J. Am. Chem. Soc. **130**, 3296 (2008).
[2] X. H. Chen, T. Wu, G. Wu, R. H. Liu, H. Chen, and D. F. Fang, Nature (London) **453**, 761 (2008).
[3] G. F. Chen, Z. Li, D. Wu, G. Li, W. Z. Hu, J. Dong, P. Zheng, J. L. Luo, and N. L. Wang, Phys. Rev. Lett. **100**, 247002 (2008).
[4] Z. A. Ren, G. C. Che, X. L. Dong, J. Yang, W. Lu, W. Yi, X. L. Shen, Z. C. Li, L. L. Sun, F. Zhou, and Z. X. Zhao, Europhys. Lett. **83**, 17002 (2008).
[5] C. Wang, L. J. Li, S. Chi, Z. W. Zhu, Z. Ren, Y. K. Li, Y. T. Wang, X. Lin, Y. K. Luo, S. Jiang, X. F. Xu, G. H. Cao, and Z. A. Xu, Europhys. Lett. **83**, 67006 (2008).
[6] H. H. Wen, G. Mu, L. Fang, H. Yang, and X. Zhu, Europhys. Lett. **82**, 17009 (2008).
[7] K. Kasperkiewicz, J. W. G. Bos, A. N. Fitch, K. Prassides, and S. Margadonna, Chem. Commun. **2009**, 707.
[8] G. Mu, B. Zeng, X. Zhu, F. Han, P. Cheng, B. Shen, and H.-H. Wen, Phys. Rev. B **79**, 104501 (2009).
[9] G. Mu, B. Zeng, P. Cheng, X. Zhu, F. Han, B. Shen, and H.-H. Wen, Europhys. Lett. **89**, 27002 (2010).
[10] G. Wu, H. Chen, Y. L. Xie, Y. J. Yan, T. Wu, R. H. Liu, X. F. Wang, D. F. Fang, J. J. Ying, and X. H. Chen, Phys. Rev. B **78**, 092503 (2008).
[11] A. S. Sefat, A. Huq, M. A. McGuire, R. Y. Jin, B. C. Sales, D. Mandrus, L. M. D. Cranswick, P. W. Stephens, and K. H. Stone, Phys. Rev. B **78**, 104505 (2008).
[12] C. Wang, Y. K. Li, Z. W. Zhu, S. Jiang, X. Lin, Y. K. Luo, S. Chi, L. J. Li, Z. Ren, M. He, H. Chen, Y. T. Wang, Q. Tao, G. H. Cao, and Z. A. Xu, Phys. Rev. B **79**, 054521 (2009).
[13] G. H. Cao, S. Jiang, X. Lin, C. Wang, Y. K. Li, Z. Ren, Q. Tao, C. M. Feng, J. H. Dai, Z. A. Xu, and F. C. Zhang, Phys. Rev. B **79**, 174505 (2009).
[14] Y. K. Li, X. Lin, T. Zhou, J. Q. Shen, Q. Tao, G. H. Cao, and Z. A. Xu, J. Phys.: Condens. Matter **21**, 355702 (2009).
[15] Y. P. Qi, L. Wang, Z. S. Gao, D. L. Wang, X. P. Zhang, Z. Y. Zhang, and Y. W. Ma, Phys. Rev. B **80**, 054502 (2009).
[16] S. Muir, A. W. Sleight, and M. A. Subramanian, Mater. Res. Bull. **45**, 392 (2010).
[17] Z. A. Ren, J. Yang, W. Lu, W. Yi, X. L. Shen, Z. C. Li, G. C. Che, X. L. Dong, L. L. Sun, F. Zhou, and Z. X. Zhao, Europhys. Lett. **82**, 57002 (2008).
[18] G. Xu, W. Ming, Y. Yao, X. Dai, S.-C. Zhang, and Z. Fang, Europhys. Lett. **82**, 67002 (2008).
[19] H. Ding, P. Richard, K. Nakayama, K. Sugawara, T. Arakane, Y. Sekiba, A. Takayama, S. Souma, T. Sato, T. Takahashi, Z. Wang, X. Dai, Z. Fang, G. F. Chen, J. L. Luo, and N. L. Wang, Europhys. Lett. **83**, 47001 (2008).
[20] K. Terashima, Y. Sekiba, J. H. Bowen, K. Nakayama, T. Kawahara, T. Sato, P. Richard, Y.-M. Xu, L. J. Li, G. H. Cao, Z. A. Xu, H. Ding, and T. Takahashi, Proc. Natl. Acad. Sci. USA **106**, 7330 (2009).
[21] X. Dai, Z. Fang, Y. Zhou, and F. C. Zhang, Phys. Rev. Lett. **101**, 057008 (2008).
[22] A. V. Chubukov, D. V. Efremov, and I. Eremin, Phys. Rev. B **78**, 134512 (2008).
[23] I. I. Mazin, D. J. Singh, M. D. Johannes, and M. H. Du, Phys. Rev. Lett. **101**, 057003 (2008).
[24] F. Wang, H. Zhai, Y. Ran, A. Vishwanath, and D. H. Lee, Phys. Rev. Lett. **102**, 047005 (2009).
[25] M. R. Presland, J. L. Tallon, R. G. Buckley, R. S. Liu, and N. E. Flower, Physica C **176**, 95 (1991).
[26] S. A. J. Kimber, D. N. Argyriou, F. Yokaichiya, K. Habicht, S. Gerischer, T. Hansen, T. Chatterji, R. Klingeler, C. Hess, G. Behr, A. Kondrat, and B. Büchner, Phys. Rev. B **78**, 140503(R) (2008).

[27] J. Zhao, Q. Huang, C. dela Cruz, J. W. Lynn, M. D. Lumsden, Z. A. Ren, J. Yang, X. Shen, X. Dong, Z. Zhao, and P. Dai, Phys. Rev. B **78**, 132504 (2008).
[28] P. M. Shirage, K. Miyazawa, H. Kito, H. Eisaki, and A. Iyo, Physica C **469**, 898 (2009).
[29] J. Prakash, S. J. Singh, D. Das, S. Patnaik, and A. K. Ganguli, J. Solid State Chem. **183**, 338 (2010).
[30] M. A. McGuire, D. J. Singh, A. S. Sefat, B. C. Sales, and D. Mandrus, J. Solid State Chem. **182**, 2326 (2009).
[31] M. Rotter, M. Tegel, and D. Johrendt, Phys. Rev. Lett. **101**, 107006 (2008).
[32] Y. J. Yan, X. F. Wang, R. H. Liu, H. Chen, Y. L. Xie, J. J. Ying, and X. H. Chen, Phys. Rev. B **81**, 235107 (2010).
[33] G. Wu, R. H. Liu, H. Chen, Y. J. Yan, T. Wu, Y. L. Xie, J. J. Ying, X. F. Wang, D. F. Fang, and X. H. Chen, Europhys. Lett. **84**, 27010 (2008).
[34] H. Chen, Y. Ren, Y. Qiu, Wei Bao, R. H. Liu, G. Wu, T. Wu, Y. L. Xie, X. F. Wang, Q. Huang, and X. H. Chen, Europhys. Lett. **85**, 17006 (2009).
[35] M. Rotter, M. Tegel, I. Schellenberg, F. M. Schappacher, R. Pötgen, J. Deisenhofer, A. Günther, F. Schrettle, A. Loidl, and D. Johrendt, New J. Phys. **11**, 025014 (2009).